



Published in final edited form as:

Stroke. 2013 November ; 44(11): . doi:10.1161/STROKEAHA.113.002073.

Deficient eNOS phosphorylation is a mechanism for diabetic vascular dysfunction contributing to increased stroke size

Qian Li, MD, PhD*, Dmitriy Atochin, MD, PhD*, Satoshi Kashiwagi, MD, PhD, John Earle, Annie Wang, MD, Emiri Mandeville, MD, PhD, Kazuhide Hayakawa, PhD, Livius V. d'Uscio, PhD, Eng H. Lo, PhD, Zvonimir Katusic, MD, PhD, William Sessa, PhD, and Paul Huang, MD, PhD

Cardiovascular Research Center (Q.L., D.A., S.K., J.E., A.W., P.H.), Neuroprotection Research Laboratory (E.M., K.H., E.H.L.), Massachusetts General Hospital and Harvard Medical School, Boston, MA; Departments of Anesthesiology and Molecular, Pharmacology, and Experimental Therapeutics, Mayo Clinic, Rochester, MN (LU, ZK), Department of Pharmacology and Vascular Biology and Therapeutics Program, Yale University School of Medicine, New Haven, CT (W.S.)

Abstract

Background and Purpose—Phosphorylation of eNOS, an important post-translational modulator of its enzymatic activity, is reduced in diabetes. We hypothesized that modulation of eNOS phosphorylation could overcome diabetic vascular dysfunction and improves the outcome to stroke.

Methods—We used the db/db mouse model of type 2 diabetes. We mated db/db mice with eNOS knockin mice that carry single-amino acid mutations at the S1176 phosphorylation site; the phosphomimetic SD mutation shows increased eNOS enzymatic activity, while the unphosphorylatable SA mutation shows decreased eNOS activity. We characterized the vascular anatomy, baseline physiologic parameters and vascular reactivity. We used the middle cerebral artery occlusion model of stroke and measured infarct volume and neurological deficits.

Results—db/db mice showed diminished eNOS phosphorylation at S1176. eNOS SD and SA mutations do not change the vascular anatomy at the Circle of Willis, brain capillary density, heart rate, or arterial blood gases of db/db mice. The eNOS SD mutation, but not the SA mutation, lowers blood pressure and improves vascular reactivity to acetylcholine in db/db mice. The eNOS SD mutation reduces stroke size and neurologic deficit following middle cerebral artery occlusion.

Conclusion—Diminished eNOS phosphorylation is a mechanism of vascular dysfunction in db/db mice. We show here that modulation of the eNOS S1176 phosphorylation site in db/db mice is associated with improved vascular reactivity and improved outcome to stroke following middle cerebral artery occlusion.

Contact person: Paul Huang, MD, PhD, Cardiovascular Research Center, Massachusetts General Hospital East, 149 Thirteenth Street, Charlestown, MA 02129, phuang1@partners.org, (617) 724-9849 phone, (617) 726-5806 fax.

*These authors contributed equally to the manuscript.

Disclosures: None.

Supplemental Material: Deficient eNOS phosphorylation is a mechanism for diabetic vascular dysfunction contributing to increased stroke size

Publisher's Disclaimer: This is a PDF file of an unedited manuscript that has been accepted for publication. As a service to our customers we are providing this early version of the manuscript. The manuscript will undergo copyediting, typesetting, and review of the resulting proof before it is published in its final citable form. Please note that during the production process errors may be discovered which could affect the content, and all legal disclaimers that apply to the journal pertain.

Keywords

nitric oxide; endothelial dysfunction; diabetes mellitus

Introduction

Cardiovascular disease, including stroke, is the major cause of morbidity and mortality in diabetes¹. The precise mechanisms of endothelial dysfunction in diabetes are not known. Here, we test the hypothesis that deficient eNOS phosphorylation is an important cause of diabetic vascular dysfunction and that its modulation can change the outcome to a disease model in vivo.

eNOS phosphorylation at serine 1177 (human sequence numbering) or its equivalents in other species, has been studied²⁻⁵. This site is phosphorylated by Akt kinase^{2, 3}, AMP kinase⁶, and protein kinase A⁷, resulting in a conformational change, enhancing electron flux through the reductase domain, and increasing NO production⁸. eNOS-derived NO plays known protective roles in cerebral ischemia, including maintenance of cerebral blood flow⁹. Models of cerebral ischemia show worse outcome with larger infarcts in eNOS knockout mice^{10, 11}. To study the effects of eNOS phosphorylation, we created eNOS knock-in mice that carry single amino acid mutations at S1176, the murine site corresponding to human S1177¹². The SD mutation (serine replaced by aspartate) results in the generation of a phosphomimetic form of eNOS with increased enzymatic activity and NO generation. The SA mutation (serine replaced by alanine) results in the generation of an unphosphorylatable form of eNOS. These mutations are located in the endogenous eNOS gene. For a mouse model of type 2 diabetes, we used the db/db mouse, which carries a point mutation in the leptin receptor gene^{13, 14}. These animals show a phenotype similar to type 2 diabetes, with hyperglycemia and insulin resistance, as well as other metabolic abnormalities^{15, 16}. We bred eNOS SD and SA mutant mice to db/db mice to test whether modulation of the eNOS S1176 phosphorylation site could overcome diabetic vascular dysfunction, and whether this affects stroke size in vivo.

Materials and Methods

Animals

Wild type (WT) and db/db mice on C57BL/6 background were obtained from Jackson laboratory. eNOS SA and SD mice were backcrossed to C57BL/6 genetic background by accelerated marker-assisted congenic breeding for 6 generations, equivalent to 10 generations of conventional breeding¹⁷. SA and SD mice were mated with db/db mice as described in Supplementary Methods. Male adult mice aged 8-17 weeks were used for all experiments (WT 12.0±3.5 weeks; db/db 12.8±1.7 weeks; SD-db/db 13.5±3.4 weeks; SA-db/db 13.3±2.7 weeks). All procedures were approved by the Massachusetts General Hospital Institutional Animal Care and Use Committee.

Biochemical and physiologic characterization

Western blotting, cGMP assay, biopterin measurements, glucose and insulin tolerance tests, microvascular density, cerebrovascular anatomy and cerebral blood flow (CBF) measurements were performed as described in Supplementary Methods. Serum lipoproteins were analyzed by HPLC¹⁸. Blood pressure was monitored in the carotid artery by blood pressure transducer (ADInstruments)¹⁸. Vessel reactivity studies were performed in a pressurized myograph system (Danish Myotechnologies)¹⁸.

Middle cerebral artery (MCA) occlusion (MCAO) model of stroke

For MCAO, a 7-0 nylon filament covered by silicon (Doccol Corp) was inserted into the internal carotid artery and advanced to the origin of the MCA for one hour, as described in Supplementary Methods.

Determination of infarct size

2 mm thick coronal brain sections were stained after 23 hours reperfusion with 2% 2, 3, 5-triphenyltetrazolium chloride (TTC)¹⁸. Total and infarcted areas were measured on the side ipsilateral to ischemia, and total area was measured on the contralateral side. Areas were integrated over the five coronal sections to obtain volumes. The percentage of the infarct volume to brain size was calculated as infarct volume divided by total volume of cerebral hemispheres without the cerebellum. To correct for edema, indirect infarct volume was calculated as volume of contralateral hemisphere minus ipsilateral non-infarcted volume.

Neurologic scoring

Mice were examined for neurologic deficits 24 hours after MCA occlusion as described¹⁹ with modifications. We excluded from original 5-point scale one point (leaning to the contralateral side), due to inability of overweight db/db, SD-db/db and SA-db/db mice to lean. Normal motor function was scored as 0, flexion of the contralateral torso and forearm on lifting the animal by the tail as 1, circling to the contralateral side as 2, and no spontaneous motor activity as 3. Measurements of infarct volume and neurological scoring were done by a blinded operator.

Statistics

All results are expressed as mean±SD. Statistical analysis was performed using Mann-Whitney test when two groups were compared, or Kruskal-Wallis test with Dunns post hoc test when more than two groups were compared. Statistical analysis for neurological deficit was performed using Kruskal-Wallis 1-way analysis of variance on ranks. Differences of $P < 0.05$ were considered significant.

Results

eNOS phosphorylation is impaired in db/db mice

We performed Western blotting to quantitate eNOS phosphorylation in the carotid artery. As seen in Figure 1, db/db mice showed normal levels of total eNOS, while eNOS phosphorylation at S1176 was diminished.

SA-db/db and SD-db/db mice

We used homologous recombination to knockin the specific SD and SA mutations into the endogenous mouse eNOS gene (Supplementary Figure IA). These mice were bred with db/db mice to obtain animals homozygous for the eNOS mutations and db/db alleles. Expression of eNOS and nNOS are the same in SD-db/db and SA-db/db mice as in WT and db/db mice (Supplementary Figure IB, C, D). eNOS mutations did not change the levels of total or phosphorylated Akt or AMP kinase (Supplementary Figure IB, E, F). The body weights of db/db (49.2 ± 5.6 g), SD-db/db (49.3 ± 7.4 g) and SA-db/db (45.9 ± 6.7 g) mice were not significantly different from each other, and were higher than WT mice (25.0 ± 3.9 g).

Cerebrovascular anatomy

We injected a latex-carbon black solution to outline the Circle of Willis and its major branches. The Circle of Willis was complete in all animals, and no redundant middle

cerebral arteries were observed. We measured the diameters of the posterior cerebral arteries (PCA) and posterior communicating (Pcomm) arteries. No significant differences were observed between WT (PCA: $138.1 \pm 27.0 \mu\text{m}$, Pcomm: $52.9 \pm 19.8 \mu\text{m}$, $n=4$), db/db (PCA: $161.4 \pm 26.6 \mu\text{m}$, Pcomm: $45.9 \pm 11.0 \mu\text{m}$, $n=5$), SA-db/db (PCA: $150.6 \pm 26.2 \mu\text{m}$, Pcomm: $66.7 \pm 34.1 \mu\text{m}$, $n=4$) and SD-db/db (PCA: $169.6 \pm 25.2 \mu\text{m}$, Pcomm: $64.4 \pm 37.4 \mu\text{m}$, $n=6$) mice (Supplementary Figure IIA and B). We measured microvascular density by lectin staining in the cerebral cortex (WT, $4.06 \pm 1.97\%$, db/db, $4.62 \pm 2.09\%$, SD-db/db $4.44 \pm 1.45\%$, SA-db/db $4.04 \pm 0.62\%$) and striatum (WT, $3.74 \pm 0.42\%$, db/db, $4.29 \pm 1.18\%$, SD-db/db $4.05 \pm 0.70\%$, SA-db/db $3.85 \pm 0.51\%$, $n=3$ per group). No significant differences were seen between any of the groups (Supplementary Figure IIC).

Metabolic parameters

Glucose tolerance and insulin tolerance testing showed impaired responses in db/db mice as compared with WT mice. The eNOS SA and SD mutations did not significantly affect the glucose tolerance and insulin tolerance curves of the db/db mice (Supplementary Figure III). Cholesterol levels were lower in WT mice compared with all other groups of mice. Triglyceride levels were not different between all groups of mice (Supplementary Table I).

SD mutation reduces stroke size in db/db mice

db/db mice show a larger stroke following MCAO than WT mice (Figure 2A, B). The percentage of the infarct volume to brain size of db/db mice was $26.5 \pm 5.0\%$, as compared to $18.0 \pm 4.9\%$ in WT mice ($n=15$, $P<0.01$). The ratio of ipsilateral to contralateral brain volumes, a reflection of brain edema, was not significantly different between db/db ($109.9 \pm 10.1\%$) and WT ($114.2 \pm 9.0\%$, $n=15$) mice. The SD mutation reduced the infarct volume of db/db mice and the percentage of infarct volume to brain ($20.2 \pm 5.8\%$, $n=12$, $P<0.05$) as compared to db/db mice. The SA mutation did not change the infarct volume or the percentage infarct volume ($25.7 \pm 4.5\%$, $n=12$) of db/db mice. The ipsilateral to contralateral brain volume ratio did not significantly differ between db/db, SD-db/db ($115.7 \pm 8.2\%$) and SA-db/db ($105.9 \pm 13.8\%$) mice. The coronal infarct areas were smaller in WT mice and SD-db/db mice compared to db/db and SA-db/db mice (Figure 2B). Together, these results show that the eNOS SD phosphomimetic mutation protects brain tissue in db/db mice, decreasing the cerebral infarct volume, with the equivalent brain edema in the mice groups. The reduction of stroke size in SD-db/db mice was associated with functional improvement, as quantitated by neurologic scoring (Figure 2C). We used laser Doppler flowmetry to assess relative CBF values in the core ischemic region. There were no significant differences between mouse groups during MCA occlusion and first 60 minutes of reperfusion (Supplementary Figure IID).

SD mutation normalized blood pressure and vascular reactivity in db/db mice

db/db mice are hypertensive compared with WT mice. The blood pressure was significantly lower in SD-db/db mice, but not in SA-db/db mice as compared with db/db mice (Figure 2D). Carotid artery vasodilation in response to ACh was impaired in db/db mice (dose response curve shifted to the right, EC_{50} $43.4 \pm 25.3 \text{ nM}$) as compared with WT mice (EC_{50} $13.1 \pm 4.9 \text{ nM}$, $p<0.01$, Figure 3A). The eNOS SD mutation improved the vascular reactivity of db/db mice, shifting the ACh dose response curve back to the left towards the WT curve. The EC_{50} for the SD-db/db mice was $10.2 \pm 5.9 \text{ nM}$ ($p<0.01$ compared with db/db mice and SA-db/db mice). In contrast, the dose response curve of SA-db/db mice was similar to the db/db mice (EC_{50} $30.0 \pm 12.3 \text{ nM}$). In response to SNP (Figure 3B), the EC_{50} for the WT mice ($8.0 \pm 4.8 \text{ nM}$) was significantly lower than SD-db/db mice ($25.8 \pm 13.8 \text{ nM}$, $P<0.05$), and not different between SD-db/db mice and db/db mice ($18.6 \pm 2.8 \text{ nM}$, $P=0.51$) or SA-db/db mice ($15.5 \pm 11.6 \text{ nM}$, $p=0.24$). Together, these results show that the eNOS SD

phosphomimetic mutation improves vascular reactivity in db/db mice, normalizing the EC₅₀ for ACh, despite reduced sensitivity of smooth muscle cells of SD-db/db mice to NO.

cGMP production and BH₄ levels

cGMP production, as a reflection of basal NO production, was decreased in aortic rings from db/db mice compared to WT mice ($P < 0.05$). SD-db/db mice showed greater cGMP production compared to db/db, SA-db/db ($P < 0.01$) mice (Figure 4A). BH₄ levels were reduced in the aortas of db/db mice as compared to WT mice (Figure 4B), while the oxidative product of BH₄, 7,8-BH₂, was not different among all studied groups (Figure 4C). The BH₄ to 7,8-BH₂ ratio was significantly decreased in db/db and SA-db/db mice aortas as compared to WT and SD-db/db mice (Figure 4D).

Discussion

Patients with type 2 diabetes display endothelial dysfunction, which is thought to play a key role in the mechanisms of atherogenesis. However, the molecular mechanisms of endothelial dysfunction are not known, nor has it been proven that improving endothelial function in diabetes will reduce cardiovascular events. Here, we use the leptin receptor deficient db/db mouse, which is a commonly used model for type 2 diabetes^{13, 14}. db/db mice develop hyperglycemia and insulin resistance and other metabolic abnormalities, including obesity and hyperlipidemia^{15, 16}. Our results demonstrate that deficient eNOS phosphorylation is a molecular mechanism of vascular dysfunction in db/db mice, and that modulation of eNOS phosphorylation corrects both vascular dysfunction and increased stroke size.

Several lines of evidence suggest that phosphorylation of eNOS at S1176 is essential to the link between metabolism and vascular dysfunction^{20, 21}. First, eNOS phosphorylation is diminished in diabetes, hypercholesterolemia and atherosclerosis. Second, estrogens, statins, and PPAR α and PPAR γ agonists increase eNOS S1176 phosphorylation. Third, vasculoprotective signaling molecules such as insulin, IGF-1, VEGF, adiponectin and leptin increase S1176 phosphorylation. These agonists act through multiple kinases to converge on eNOS phosphorylation, suggesting that this is a common integration point that underlies endothelial dysfunction from various causes.

To study the effects of phosphorylation, we used single amino acid eNOS mutations at S1176. In the SD mutation, serine is replaced by aspartate, which has a negatively charged carboxyl group. The negative charge and the size of the side chain are similar to the negatively charged phosphate group of phospho-eNOS, hence the designation of the mutation as phosphomimetic. In contrast, the SA mutation replaces serine with alanine, of which the methyl side chain is unphosphorylatable. These mutations have been characterized in vitro, and are known to affect eNOS enzymatic activity, with the SD mutation showing increased NO production at rest and the SA mutation showing decreased NO production^{2, 3}. Both mutations are sensitive to calcium stimulation, and the SA mutation is not a null mutation.

In this study, we used eNOS SD and SA knockin mice in which the endogenous eNOS gene carries these single amino acid mutations. We bred these mice to db/db mice to study vascular function and outcome to stroke. In the MCA occlusion model of stroke, the quantitative endpoint is the infarct volume. A meaningful comparison presupposes that the territories at risk are comparable, and that the effects of the filament occlusion are the same. We sought to address these issues in several ways. First, we assessed the effects of the eNOS mutations on cerebrovascular anatomy relevant to the outcome of the stroke model. We performed carbon black injections to visualize the vessels and to ensure that continuity of the Circle of Willis was not affected. We did not observe redundant MCA or changes in

the sizes of the PCA or Pcomm arteries that would affect outcome to filament occlusion. We performed lectin staining to quantitate capillary density and ensure that there were no detectable differences that may affect the stroke volume. Second, we assessed absolute CBF in the animals by hydrogen clearance. Third, we calculated infarct volume in several ways: direct infarct volume, indirect infarct volume, which accounts for ipsilateral edema, and percent infarct volume to brain size, which accounts for differences in brain size. Using all of these measures, the SD mutation reduced the infarct size of db/db mice, while the SA mutation did not. Fourth, we verified by laser Doppler flowmetry that the filament caused the same CBF reductions in the core ischemic zone.

Improvements in CBF in the ischemic penumbra are the most likely mechanism for the eNOS SD mutation to reduce infarct size in db/db mice¹¹. In support of this, we found that the impaired vascular reactivity in db/db mice is improved by the SD mutation but not the SA mutation.

We wish to point out potential limitations of our study. In addition to vascular effects, eNOS-derived NO is known to inhibit platelet aggregation and adhesion²², and block leukocyte-endothelial interactions²³. Although we demonstrate that the SD mutation improves vascular reactivity, we did not examine whether the SD mutation also acts through alterations of hemostasis, inflammation, or other effects. These systemic effects, either in the CNS or other organ systems, may also affect the outcome to cerebral ischemia. Thus, the effects of eNOS phosphorylation may not be exclusively vascular.

eNOS has been reported to affect insulin sensitivity, and high fat-fed eNOS knockout mice display insulin resistance²⁴. We performed glucose tolerance tests, insulin tolerance tests, and measured lipid profiles. The eNOS SD and SA mutations do not significantly affect these metabolic parameters in db/db mice. We measured BH₄, which is important to prevent eNOS uncoupling²⁵. The ratio of BH₄/BH₂ is significantly reduced in db/db mice as compared to WT mice, but it is the same in SD-db/db mice as WT mice. This could occur by upregulation of GTP cyclohydrolase I expression, the rate-limiting step in BH₄ production²⁶. It is still possible that there are other metabolic effects of eNOS mutations that could alter the outcome to cerebral ischemia. Alternatively, the eNOS mutations and the db/db mutation may both influence stroke size, but through mechanisms unique to one or the other that do not overlap.

We confirmed the functional significance of the reduced cerebral infarct size by neurologic scoring, using a system tailored for mice¹⁹ modified for body habitus. Like the Bederson score developed for use in rats²⁷, it includes forelimb flexion and circling behavior, but it differs because it does not include lateral push which is a less reliable indicator in overweight mice, and it does include absence of spontaneous activity as an indicator of severe neurologic functional deficit.

We previously reported that eNOS knockout mice that carry mutant bovine eNOSS1179 transgenes (bovine numbering corresponding to S1177 in humans and S1176 in mice) could be used to study the effects of those mutations on an eNOS-null background. The current study differs from the previous report in several important ways. First, we are here using knockin mice in which the endogenous eNOS gene is mutated, rather than transgenic mice. Thus, effects due to expression level, transgene copy number, and site of integration are avoided. Second, we are assessing the effects of the eNOS mutations on the phenotype of the db/db mice in the stroke model, not the effects of the mutations by themselves.

Because NO needs to be generated in the proper subcellular location and with precise timing²⁸, targeting phosphorylation of the endogenous eNOS enzyme offers advantages over pharmacologic replacement of NO with nitrate donors or genetic overexpression of

endothelial or other NOS isoforms by gene therapy. The appropriate targets for modulation of NO production by eNOS may be the kinases or phosphatases that regulate eNOS phosphorylation. In addition to eNOS phosphorylation, Akt kinase, AMPK, and PKA clearly have other substrates and effects that may impact cell survival.

Conclusion

db/db mice show diminished eNOS phosphorylation, greater stroke size following MCAO, hypertension and impaired vascular reactivity. The phosphomimetic eNOS SD mutation improves NO production, reduces stroke size, corrects hypertension and improves vascular reactivity. These results demonstrate that modulation of the eNOS phosphorylation site in db/db mice has beneficial effects on physiology and outcome to a stroke model.

Supplementary Material

Refer to Web version on PubMed Central for supplementary material.

Acknowledgments

We are grateful to Helen Swanson for technical assistance.

Funding Sources: This work was supported by NIH R01 HL57818 and NS33335 to PLH and American Heart Association Scientist Development Grant 0835344N to DNA.

References

1. Grundy SM, Benjamin IJ, Burke GL, Chait A, Eckel RH, Howard BV, et al. Diabetes and cardiovascular disease: A statement for healthcare professionals from the American Heart Association. *Circulation*. 1999; 100:1134–1146. [PubMed: 10477542]
2. Dimmeler S, Fleming I, Fisslthaler B, Hermann C, Busse R, Zeiher AM. Activation of nitric oxide synthase in endothelial cells by akt-dependent phosphorylation. *Nature*. 1999; 399:601–605. [PubMed: 10376603]
3. Fulton D, Gratton JP, McCabe TJ, Fontana J, Fujio Y, Walsh K, et al. Regulation of endothelium-derived nitric oxide production by the protein kinase akt. *Nature*. 1999; 399:597–601. [PubMed: 10376602]
4. Harris MB, Ju H, Venema VJ, Liang H, Zou R, Michell BJ, et al. Reciprocal phosphorylation and regulation of endothelial nitric-oxide synthase in response to bradykinin stimulation. *J Biol Chem*. 2001; 276:16587–16591. [PubMed: 11340086]
5. Michell BJ, Chen Z, Tiganis T, Stapleton D, Katsis F, Power DA, et al. Coordinated control of endothelial nitric-oxide synthase phosphorylation by protein kinase c and the camp-dependent protein kinase. *J Biol Chem*. 2001; 276:17625–17628. [PubMed: 11292821]
6. Chen ZP, Mitchelhill KI, Michell BJ, Stapleton D, Rodriguez-Crespo I, Witters LA, et al. Amp-activated protein kinase phosphorylation of endothelial nitric oxide synthase. *FEBS Lett*. 1999; 443:285–289. [PubMed: 10025949]
7. Butt E, Bernhardt M, Smolenski A, Kotsonis P, Frohlich LG, Sickmann A, et al. Endothelial nitric-oxide synthase (type iii) is activated and becomes calcium independent upon phosphorylation by cyclic nucleotide-dependent protein kinases. *J Biol Chem*. 2000; 275:5179–5187. [PubMed: 10671564]
8. McCabe TJ, Fulton D, Roman LJ, Sessa WC. Enhanced electron flux and reduced calmodulin dissociation may explain “Calcium-independent” Enos activation by phosphorylation. *J Biol Chem*. 2000; 275:6123–6128. [PubMed: 10692402]
9. Endres M, Laufs U, Liao JK, Moskowitz MA. Targeting enos for stroke protection. *Trends Neurosci*. 2004; 27:283–289. [PubMed: 15111011]

10. Huang Z, Huang PL, Ma J, Meng W, Ayata C, Fishman MC, et al. Enlarged infarcts in endothelial nitric oxide synthase knockout mice are attenuated by nitro-L-arginine. *J Cereb Blood Flow Metab.* 1996; 16:981–987. [PubMed: 8784243]
11. Lo EH, Hara H, Rogowska J, Trocha M, Pierce AR, Huang PL, et al. Temporal correlation mapping analysis of the hemodynamic penumbra in mutant mice deficient in endothelial nitric oxide synthase gene expression. *Stroke.* 1996; 27:1381–1385. [PubMed: 8711806]
12. Kashiwagi S, Atochin DN, Li Q, Schleicher M, Pong T, Sessa WC, et al. Enos phosphorylation on serine 1176 affects insulin sensitivity and adiposity. *Biochem Biophys Res Commun.* 2013; 431:284–290. [PubMed: 23291238]
13. Coleman DL. Obese and diabetes: Two mutant genes causing diabetes-obesity syndromes in mice. *Diabetologia.* 1978; 14:141–148. [PubMed: 350680]
14. Coleman DL. A historical perspective on leptin. *Nat Med.* 2010; 16:1097–1099. [PubMed: 20930752]
15. Chen H, Charlat O, Tartaglia LA, Woolf EA, Weng X, Ellis SJ, et al. Evidence that the diabetes gene encodes the leptin receptor: Identification of a mutation in the leptin receptor gene in db/db mice. *Cell.* 1996; 84:491–495. [PubMed: 8608603]
16. Hummel KP, Dickie MM, Coleman DL. Diabetes, a new mutation in the mouse. *Science.* 1966; 153:1127–1128. [PubMed: 5918576]
17. Markel P, Shu P, Ebeling C, Carlson GA, Nagle DL, Smutko JS, et al. Theoretical and empirical issues for marker-assisted breeding of congenic mouse strains. *Nat Genet.* 1997; 17:280–284. [PubMed: 9354790]
18. Atochin DN, Wang A, Liu VW, Critchlow JD, Dantas AP, Looft-Wilson R, et al. The phosphorylation state of enos modulates vascular reactivity and outcome of cerebral ischemia in vivo. *J Clin Invest.* 2007; 117:1961–1967. [PubMed: 17557122]
19. Huang Z, Huang PL, Panahian N, Dalkara T, Fishman MC, Moskowitz MA. Effects of cerebral ischemia in mice deficient in neuronal nitric oxide synthase. *Science.* 1994; 265:1883–1885. [PubMed: 7522345]
20. Huang PL. eNOS, metabolic syndrome and cardiovascular disease. *Trends Endocrinol Metab.* 2009; 20:295–302. [PubMed: 19647446]
21. Huang PL. A comprehensive definition for metabolic syndrome. *Dis Model Mech.* 2009; 2:231–237. [PubMed: 19407331]
22. Freedman JE, Sauter R, Battinelli EM, Ault K, Knowles C, Huang PL, et al. Deficient platelet-derived nitric oxide and enhanced hemostasis in mice lacking the nosiii gene. *Circ Res.* 1999; 84:1416–1421. [PubMed: 10381894]
23. Lefer DJ, Jones SP, Girod WG, Baines A, Grisham MB, Cockrell AS, et al. Leukocyte-endothelial cell interactions in nitric oxide synthase-deficient mice. *Am J Physiol.* 1999; 276:H1943–1950. [PubMed: 10362674]
24. Duplain H, Burcelin R, Sartori C, Cook S, Egli M, Lepori M, et al. Insulin resistance, hyperlipidemia, and hypertension in mice lacking endothelial nitric oxide synthase. *Circulation.* 2001; 104:342–345. [PubMed: 11457755]
25. Katusic ZS, d'Uscio LV, Nath KA. Vascular protection by tetrahydrobiopterin: Progress and therapeutic prospects. *Trends Pharmacol Sci.* 2009; 30:48–54. [PubMed: 19042039]
26. Kumar S, Sun X, Sharma S, Aggarwal S, Ravi K, Fineman JR, et al. Gtp cyclohydrolase i expression is regulated by nitric oxide: Role of cyclic amp. *Am J Physiol Lung Cell Mol Physiol.* 2009; 297:L309–317. [PubMed: 19447893]
27. Bederson JB, Pitts LH, Tsuji M, Nishimura MC, Davis RL, Bartkowski H. Rat middle cerebral artery occlusion: Evaluation of the model and development of a neurologic examination. *Stroke.* 1986; 17:472–476. [PubMed: 3715945]
28. Dudzinski DM, Igarashi J, Greif D, Michel T. The regulation and pharmacology of endothelial nitric oxide synthase. *Annu Rev Pharmacol Toxicol.* 2006; 46:235–276. [PubMed: 16402905]

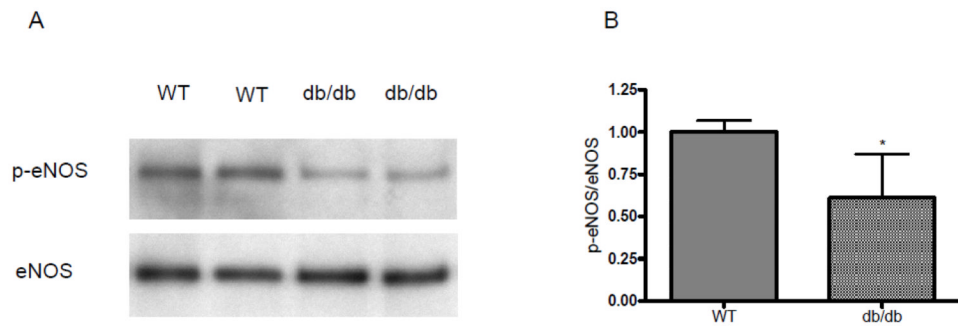


Figure 1. eNOS phosphorylation in the carotid artery of WT and db/db mice

A. Representative Western blot probed with antibody to p-eNOS and total eNOS. B. Densitometry (n=8 each group). *P<0.05, WT vs. db/db.

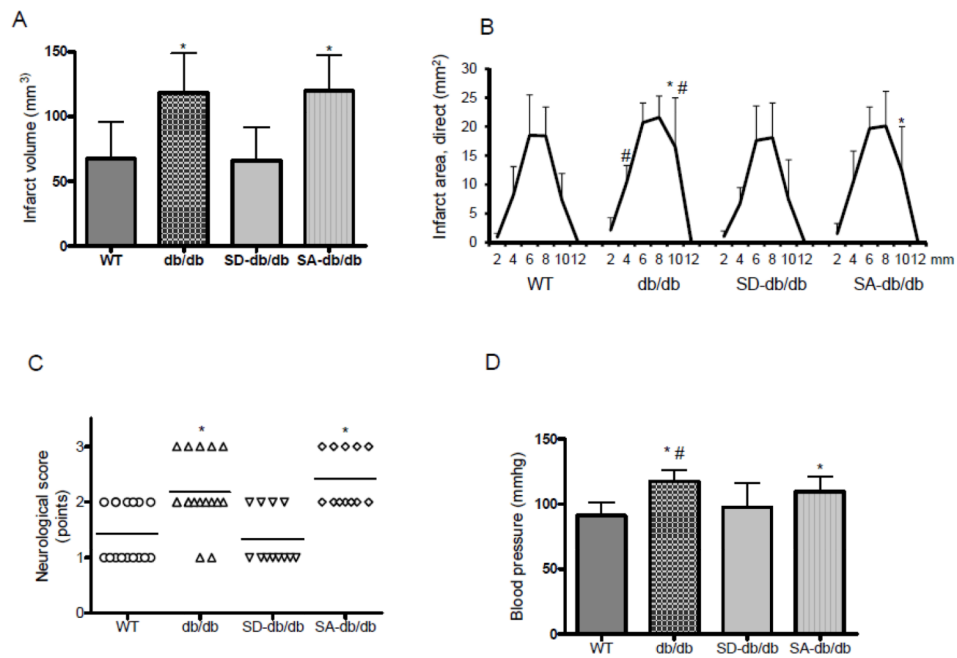


Figure 2. Cerebral infarct volumes, neurological score, and infarct areas

A. Indirect cerebral infarct volumes (mm³) 23 hours after reperfusion. (n=15, WT and db/db; n=12, SD-db/db and SA-db/db mice. *P<0.01 vs. WT and SD-db/db). B. Infarct areas (mm²) for each coronal section. (*P<0.01 vs. WT and #P<0.01 vs. SD-db/db). C. Neurological scores. (n=15, WT and db/db; n=12, SD-db/db; n=11, SA-db/db mice. *P<0.01 vs. WT and SD-db/db). D. Mean arterial blood pressure (n=15 each group). *P<0.01 vs. WT and #P<0.01 vs. SD-db/db.

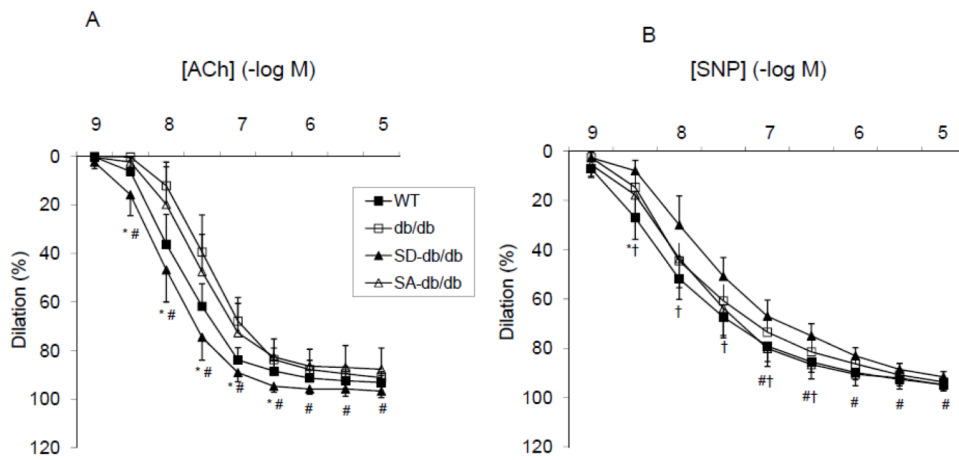


Figure 3. Effect of eNOS mutations on vascular reactivity

A. Dose response curves to ACh. WT (n=18); db/db (n=17); SD-db/db (n=6); SA-db/db (n=6). *P<0.05 WT vs. db/db; #P<0.05 SD-db/db vs. db/db and SA-db/db. B. Dose response curves to SNP. WT (n=12); db/db (n=17); SD-db/db (n=6); SA-db/db (n=5). *P<0.05 WT vs. db/db; †P<0.05 WT vs. SD-db/db; #P<0.05 SD-db/db vs. SA-db/db

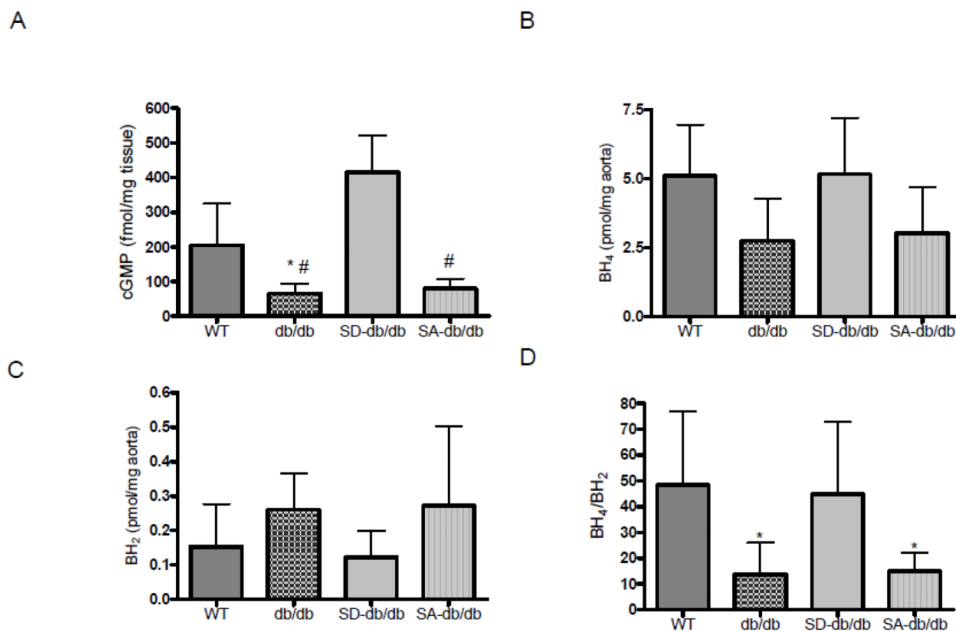


Figure 4. cGMP and biopterin levels

A. cGMP levels in aorta: WT (n=8), db/db (n=6), SD-db/db (n=6) and SA-db/db (n=4) mice. *P<0.05, db/db vs. WT; #P<0.01, db/db and SA-db/db vs. SD-db/db. B. BH₄ levels. C. BH₂ levels. D. BH₄/BH₂ratio. Measurements were made in aorta of WT (n=7), db/db (n=5), SD-db/db (n=6) and SA-db/db (n=7) mice. *P<0.05, db/db and SA-db/db vs. WT and SD-db/db.